

# Oscillatory Quadrupole-like Expansion of a Fermionic Superfluid

Yu-Ping Wu,<sup>1,2,3</sup> Xing-Can Yao,<sup>1,2,3</sup> Xiang-Pei Liu,<sup>1,2,3</sup> Xiao-Qiong Wang,<sup>1,2,3</sup> Yu-Xuan Wang,<sup>1,2,3</sup>  
Hao-Ze Chen,<sup>1,2,3</sup> Mudassar Maraj,<sup>1,2,3</sup> Youjin Deng,<sup>1,2,3</sup> Yu-Ao Chen,<sup>1,2,3</sup> and Jian-Wei Pan<sup>1,2,3</sup>

<sup>1</sup>*Shanghai Branch, National Laboratory for Physical Sciences at Microscale and Department of Modern Physics, University of Science and Technology of China, Shanghai, 201315, China*

<sup>2</sup>*CAS Center for Excellence and Synergetic Innovation Center in Quantum Information and Quantum Physics, University of Science and Technology of China, Hefei, Anhui 230026, China*

<sup>3</sup>*CAS-Alibaba Quantum Computing Laboratory, Shanghai, 201315, China*

We prepare a Fermionic superfluid of about  $5 \times 10^6$   $^6\text{Li}$  atoms in a cigar-shaped optical dipole trap and demonstrate that in the weak residual magnetic field curvature, the atom cloud undergoes an oscillatory quadrupole-like expansion over 30 ms. By analyzing the expansion dynamics according to the superfluid hydrodynamic equation, we derive several parameters characterizing quantum state of the trapped Fermionic superfluid, including the Bertsch parameter  $\xi$  at unitarity and the effective polytropic index  $\bar{\gamma}$  over the whole BEC-BCS crossover. The experimental estimate  $\xi = 0.42(2)$  agrees well with the quantum Monte Carlo calculation 0.42(1). The  $\bar{\gamma}$  values show a nonmonotonic behavior as a function of interaction strength, and reduce to the well-known theoretical results in the BEC, BCS and unitary limits.

PACS numbers: 03.67.-a

With an exquisite control of interaction strength and other physical parameters [1, 2], degenerate Fermi gas (DFG) has become a versatile platform to study a wide variety of fundamental questions and phenomena, ranging from high-temperature superconductor, neutron star to quark-gluon plasma of the early Universe [3, 4]. Important experimental progresses include realization of molecular Bose-Einstein condensate (BEC) [5, 6], generation of vortices in a rotating Fermi gas as a conclusive evidence of Fermionic superfluidity [7, 8], and precise study of superfluid phase transition and universal properties via direct measurement of the equation-of-state (EoS) of DFG [9–12] etc.

Among various techniques for gaining information on the properties of DFG, measurements on expansion dynamics of atom cloud released from trap are established to be a powerful tool [13–15]. Hydrodynamic behaviors [13] are well revealed and the interaction energy of DFG is obtained in the BEC-BCS crossover [16]. Collective effect is observed in hydrodynamic expansion of a strongly interacting Fermi-Fermi mixture [15]. Very recently, shear viscosity [17–19], conformal symmetry breaking and scale invariance [20] are explored during the study of expansion of DFG. However, the expansion time of DFG is limited to a few milliseconds [13, 15, 19], preventing observation of various interesting and important phenomena. In particular, long-time quadrupole-like expansion predicted by the superfluid hydrodynamic equation has not been achieved [14].

In this Letter, we prepare a Fermionic superfluid of about  $5 \times 10^6$   $^6\text{Li}$  atoms at temperature  $T/T_F = 0.06(1)$  in a cigar-shaped optical dipole trap, with  $T_F$  the Fermi temperature. By suddenly switching off the optical trap, we observe a quadrupole-like expansion of the superfluid in the weak residual magnetic field curvature, persisting

for a long time of more than 30 ms. A pronounced feature is that the anisotropic atom cloud displays an oscillatory expansion behavior; namely, the cloud sizes in the radial and axial directions oscillate during expansion.

The expansion dynamics is qualitatively consistent with the numerical solution of a hydrodynamic equation of motion for trapped superfluid, and quantitative agreement is further observed during the first several milliseconds of expansion. From a least-squares-criterion fitting, we obtain several parameters characterizing quantum state of the trapped Fermionic superfluid. The so-called Bertsch parameter  $\xi$  at unitarity is determined to be  $\xi = 0.42(2)$ , in an excellent agreement with a fixed-node quantum Monte-Carlo calculation 0.42(1) [21]. The results for the effective polytropic index  $\bar{\gamma}$  of EoS are obtained over the whole BEC-BCS crossover, and is found to display a nonmonotonic behavior as a function of interaction strength [14, 22]. In the BEC, BCS and unitary limits, the  $\bar{\gamma}$  values are well consistent with the well-known theoretical predictions. The long-life oscillatory expansion dynamics and the successful derivation of quantitative informations can be attributed to the large atom number and the sufficiently low temperature of the prepared Fermionic superfluid. Our work serves as an example towards high-precision study of static and dynamic properties of DFG.

**Oscillatory expansion at unitarity.** The experimental setup has been described in our previous works [23–25]. We start with a mixture of  $^6\text{Li}$  and  $^{41}\text{K}$  atoms in an optically-plugged magnetic trap, where the  $^6\text{Li}$  atoms are sympathetically cooled by the  $^{41}\text{K}$  atoms. After the final radio-frequency (rf) "knife" of evaporation [26], the  $^{41}\text{K}$  atoms are exhausted and a pure  $^6\text{Li}$  cloud is prepared. Then about  $2 \times 10^7$   $^6\text{Li}$  atoms with a temperature of about 50  $\mu\text{K}$  are loaded into the cigar-

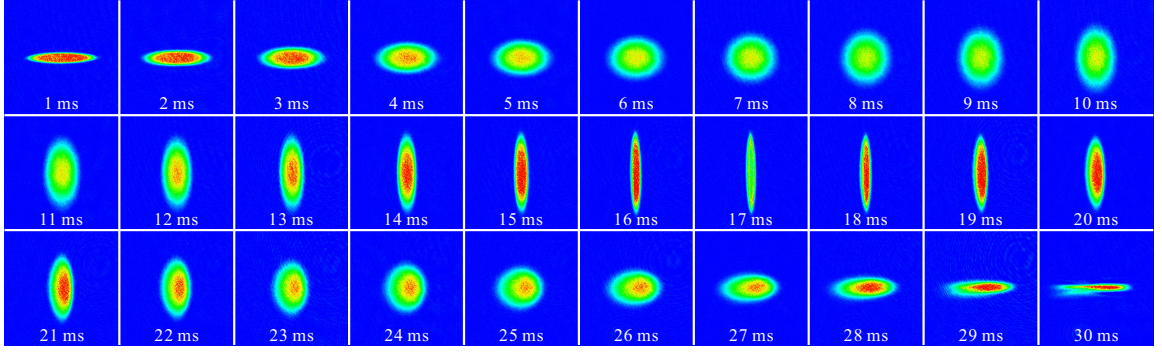


FIG. 1. Quadrupole-like expansion of  ${}^6\text{Li}$  superfluid at 834 G. Each picture has a field of view of 1.3 mm $\times$ 1.3 mm.

shaped optical dipole trap (wavelength 1064 nm,  $1/e^2$  beam waist 64  $\mu\text{m}$ ) and immediately transferred to the lowest hyperfine state by a 3 ms Landau-Zener sweep [27]. Next, we adiabatically ramp the magnetic field  $B$  to the unitary point with  $B = 834$  G, and apply several rf pulses to prepare a balanced mixture of the two lowest hyperfine states. Forced evaporative cooling is accomplished by exponentially reducing the depth of the dipole trap. After a 3 s evaporation, about  $5 \times 10^6$   ${}^6\text{Li}$  atoms at temperature  $T/T_F = 0.06(1)$  are prepared. The radial confinement is mainly optical with final trap frequencies of  $\omega_y = 2\pi \times 211.9$  Hz and  $\omega_z = 2\pi \times 200.1$  Hz, where  $y$  is the radial direction in the horizontal plane and  $z$  is the gravity direction. The axial confinement ( $x$  direction) is mainly provided by the magnetic field curvature with a trap frequency  $\omega_x = 2\pi \times 16.5$  Hz at 834 G.

Before expansion, the  ${}^6\text{Li}$  superfluid cloud is held for another 400 ms to achieve fully thermal equilibrium. Then the optical dipole trap is abruptly switched off and the  ${}^6\text{Li}$  cloud is expanded in the residual magnetic field curvature. To minimize the asymmetric effect caused by the repulsive potential in  $z$  direction, a magnetic field gradient of  $\partial_z B = 1.1$  G/cm is simultaneously turned on to levitate the superfluid at the saddle point. An imaging system with resolution of 2.2  $\mu\text{m}$  is employed to obtain high quality images [23]. The experimental results are shown in Fig. 1, where pictures are taken at a time interval of 1 ms. Thanks to the large atom number of the prepared  ${}^6\text{Li}$  superfluid, an oscillatory quadrupole-like expansion persists for a long time of over 30 ms, during which the cloud sizes in the radial and axial directions both oscillate as a function of expansion time  $t$ . This is unlike ballistic or anisotropic expansion in Refs. [13, 17], where atom cloud keeps expanding. The oscillatory behavior can be characterized by the aspect ratio  $R_y(t)/R_x(t)$ , where  $R_x(t)$  and  $R_y(t)$  are respectively the radii in the  $x$  and  $y$  directions. With an initial value of 0.078 at  $t = 0$ , the aspect ratio increases, reaches a maximum value of 8.5 at time  $t_0 \sim 17$  ms, and gradually decreases after  $t_0$ . We define quantity  $f_0 \equiv 1/2t_0$  as quasi-frequency of the oscillatory ex-

pansion and  $A_0 \equiv \frac{R_y(t_0)}{R_x(t_0)} / \frac{R_x(0)}{R_y(0)}$  as the normalized quasi-amplitude.

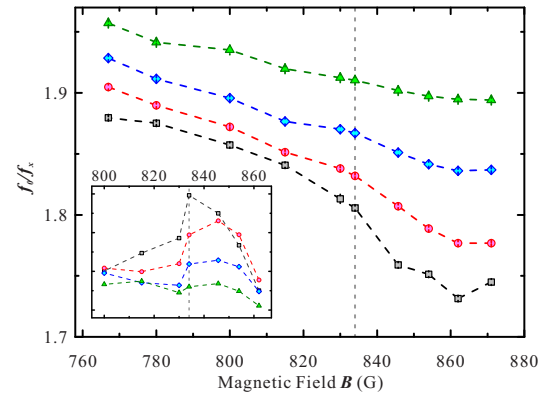


FIG. 2. Normalized quasi-frequency  $f_0/f_x$  versus bias magnetic field. Results represented by gray square, red circle, blue diamond, and green triangle are for  $T/T_F$  of 0.06(1), 0.13(3), 0.18(2), and 0.27(4), respectively. The vertical dash-dotted line marks the position of Feshbach resonance. The inset shows the absolute slope  $|(1/f_x)(\delta f_0/\delta B)|$ , as derived from the neighboring data points.

### Oscillatory expansion at BEC-BCS crossover.

With the same procedure, oscillatory quadrupole-like expansions are observed in the whole BEC-BCS crossover and for various temperatures  $T$ . The quasi-frequency  $f_0$  is recorded and normalized by the  $B$ -dependent residual frequency  $f_x = \omega_x/2\pi$ . The results in Fig. 2 show that the normalized quasi-frequency  $f_0/f_x$  drops significantly from the BEC side to the BCS side and reaches a minimum around 860 G, particularly at low temperatures. As  $T$  goes up, the normalized quasi-amplitude  $A_0$  of the oscillatory expansion decreases from 49% ( $T/T_F = 0.13(3)$ ) to 25% ( $T/T_F = 0.27(4)$ ), and the  $B$ -dependence of normalized quasi-frequency  $f_0/f_x$  is smoothed out. The absolute slope  $|(1/f_x)(\delta f_0/\delta B)|$ , calculated from a pair of neighboring data points, roughly has a bump near the resonance at low temperature (the inset of Fig. 2). For  $T > 0.18(2)T_F$ , the bump is significantly suppressed, implying that the cloud might mostly consist of thermal

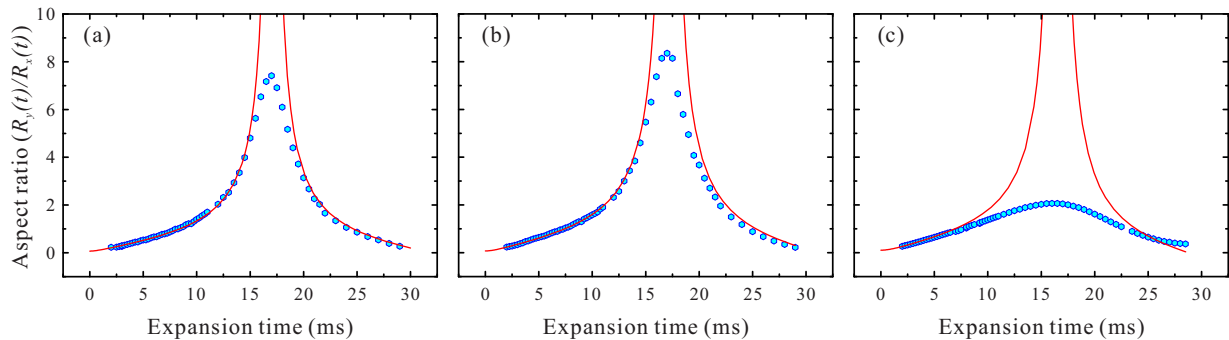


FIG. 3. Aspect ratio versus expansion time. Blue dots in (a), (b), and (c) are experiment results taken at 767 G, 834 G, and 1003.2 G, respectively, while red solid lines are theoretical predictions of Eq. 1 with  $\bar{\gamma} = 1$ ,  $\bar{\gamma} = 2/3$ , and  $\bar{\gamma} = 2/3$ , respectively.

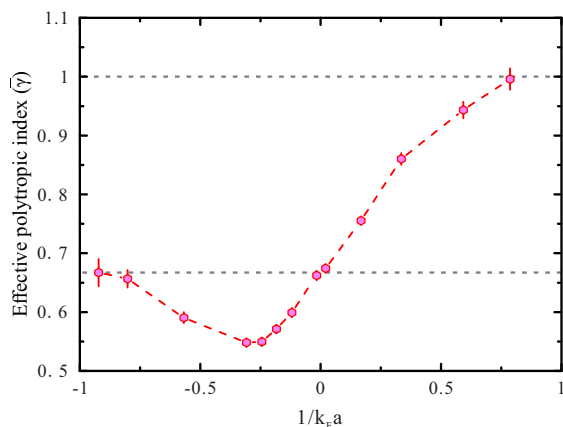


FIG. 4. Effective polytropic index versus interaction strength. Horizontal dash-dotted lines mark the theoretical predictions in the limiting cases.

atoms. We note that in Ref. [28], the breathing-mode frequency of a trapped Fermi  $^6\text{Li}$  gas is observed to display a similar  $B$ -dependence as the curve of  $f_0/f_x$  in Fig. 2; the measurements in Ref. [28] are very precise, and beyond-mean-field effects are accurately extracted and found to be consistent with quantum Monte Carlo calculation.

**Quantitative analysis.** To quantitatively analyze the expansion dynamics, detailed knowledge of EoS of  $^6\text{Li}$  superfluid is required. We take an often-adopted "polytropic" form of EoS [22, 29, 30],  $\mu(r) \propto n(r)^\gamma$ , relating the local chemical potential  $\mu(r)$  to the local density  $n(r)$ . The polytropic index  $\gamma$  is governed by the interaction strength  $1/k_F a$  ( $k_F$  is the Fermi momentum and  $a$  is the scattering length). On this basis, the superfluid hydrodynamic equation is obtained

$$\ddot{b}_i(t) = -\omega_i^2(t > 0)b_i(t) + \frac{\omega_i^2(t < 0)}{b_i(t)V(t)^{\bar{\gamma}}} \quad (1)$$

where  $i = x, y, z$ ,  $b_i(t) = R_i(t)/R_i(0)$  is the normalized radius,  $V(t) = \prod_i b_i(t)$ , and effective polytropic index  $\bar{\gamma}$  is trap-dependent. In the BEC limit ( $1/k_F a \gg 1$ ) one has  $\mu(r) \propto n(r)$  and thus  $\bar{\gamma} = 1$ , while in the BCS limit

( $1/k_F a \ll -1$ ) and the unitary limit ( $1/k_F a = 0$ ),  $\mu(r) \propto n(r)^{2/3}$  leads to  $\bar{\gamma} = 2/3$ .

Figure 3 shows the experimental results of the aspect ratio  $R_y(t)/R_x(t)$  at 767 G (deep BEC side), 834 G (unitary) and 1003.2 G (deep BCS side). Also shown are the numerical solutions of Eq. (1) (red lines), where the known  $\bar{\gamma}$  values have been used. Quantitative agreement is found during the early stage of expansion and up to a long time of over 11 ms on the BEC side and at unitarity; the agreement is up to 6 ms on the BCS side, where fragile pairs might break during expansion. Afterward, the general trends still agree qualitatively, while large deviations occur around the turning point, where the superfluid becomes a quasi-2D cloud and surface tension effect cannot be simply neglected.

At unitarity, the so-called Bertsch parameter  $\xi$  is an important parameter characterizing the trapped superfluid. It is known that the cloud radius  $R_x(0)$  and the Thomas-Fermi radius  $R_{Fx}$  are related as  $R_x(0) = \xi^{1/4} R_{Fx}$  [4, 14]. During expansion, the superfluid cloud becomes less saturated and the measured radius  $R_x(t)$  by absorption imaging is expected to be more precise. Making use of the quantitative agreement of the early expansion, we extract the initial radius  $R_x(0) = 0.418(5)$  mm from the least-squares-criterion fitting of  $R_x(t)$  with  $t \leq 11$  ms. Together with the experimental measurement  $R_{Fx} = 0.519(5)$  mm, we determine  $\xi = 0.42(2)$ , in an excellent agreement with the fixed-node quantum Monte Carlo calculation 0.42(1) [21]. We also mention that the experimental result of the normalized quasi-frequency  $f_0/f_x = 1.80$  in Fig. 2 agrees well with the numerical solution of Eq. (1), which gives  $f_0/f_x = 1.77$ .

Quantitative analyses are then carried out for the strongly interacting regime ( $1/k_F |a| < 1$ ), where  $\bar{\gamma}$  is unknown. We fine tune the  $\bar{\gamma}$  value in Eq. (1) such that the numerical solution fits the experimental data with  $t \leq 11$  ms for  $1/k_F a > -0.3$  and  $t \leq 6$  ms for  $1/k_F a \leq -0.3$ . The results of  $\bar{\gamma}$  are shown in Fig. 4, with standard deviations less than 3.5%. The  $\bar{\gamma}$  value smoothly decreases from the BEC to BCS side, reaches a minimum value of 0.55(1) at  $1/k_F a \approx -0.27$ , and then

gradually increases to the theoretical value  $2/3$  in the BCS limit. Our results are consistent with the theoretical predictions in Ref. [14, 22].

In summary, we successfully demonstrate that in the weak residual magnetic field curvature, an anisotropic Fermionic superfluid cloud experiences an oscillatory quadrupole-like expansion for over 30 ms. The oscillatory behavior is well supported by a superfluid hydrodynamic equation, and quantitative agreement is found during the early stage of expansion up to 11 ms. To sustain such a long time of expansion and oscillatory behavior, a large atom number of the atom cloud ( $5 \times 10^6$  in this work) is needed. Further, we extract the radius of the trapped superfluid from the first several milliseconds of expansion and obtain the Bertsch parameter  $0.42(2)$ . The excellent agreement with the quantum Monte Carlo calculation  $0.42(1)$  implies this simple method can be reliably used to estimate the cloud size. The effective polytropic index of EoS is also determined for the whole BEC-BCS crossover, and is found to be consistent with the numerical calculations in Ref. [14, 22]. We expect that with large atom number and low temperature, high-precision study of many interesting static and dynamic phenomena in Fermionic superfluid becomes promising, which include elliptic flow [15, 17], normal-superfluid phase transition [31], and super-Efimov effect [32–34] etc.

We are indebted to valuable discussions with Q.-J. Chen and H. Zhai. This work has been supported by the NSFC of China, the CAS, and the National Fundamental Research Program (under Grant Nos. 2013CB922001 and 2016YFA0301600). Y.-P. Wu and X.-C. Yao contributed equally to this work.

- 
- [1] C. Chin, R. Grimm, P. Julienne, and E. Tiesinga, *Rev. Mod. Phys.* **82**, 1225 (2010).
  - [2] K. Dieckmann, C. A. Stan, S. Gupta, Z. Hadzibabic, C. H. Schunck, and W. Ketterle, *Phys. Rev. Lett.* **89**, 203201 (2002).
  - [3] I. Bloch, J. Dalibard, and W. Zwerger, *Rev. Mod. Phys.* **80**, 885 (2008).
  - [4] S. Giorgini, L. P. Pitaevskii, and S. Stringari, *Rev. Mod. Phys.* **80**, 1215 (2008).
  - [5] M. Greiner, C. A. Regal, and D. S. Jin, *Nature* **426**, 537 (2003).
  - [6] S. Jochim, M. Bartenstein, A. Altmeyer, G. Hendl, S. Riedl, C. Chin, J. Hecker Denschlag, and R. Grimm, *Science* **302**, 2101 (2003).
  - [7] M. W. Zwierlein, J. R. Abo-Shaeer, A. Schirotzek, C. H. Schunck, and W. Ketterle, *Nature* **435**, 1047 (2005).
  - [8] M. W. Zwierlein, A. Schirotzek, C. H. Schunck, and W. Ketterle, *Science* **311**, 492 (2006).
  - [9] S. Nascimbène, N. Navon, K. J. Jiang, F. Chevy, and C. Salomon, *Nature* **463**, 1057 (2010).
  - [10] N. Navon, S. Nascimbène, F. Chevy, and C. Salomon, *Science* **328**, 729 (2010).
  - [11] M. Horikoshi, S. Nakajima, M. Ueda, and T. Mukaiyama, *Science* **327**, 442 (2010).
  - [12] M. J. H. Ku, A. T. Sommer, L. W. Cheuk, and M. W. Zwierlein, *Science* **335**, 563 (2012).
  - [13] K. M. O'Hara, S. L. Hemmer, M. E. Gehm, S. R. Granade, and J. E. Thomas, *Science* **298**, 2179 (2002).
  - [14] W. Ketterle and M. W. Zwierlein, arXiv preprint arXiv:0801.2500 (2008).
  - [15] A. Trenkwalder, C. Kohstall, M. Zaccanti, D. Naik, A. I. Sidorov, F. Schreck, and R. Grimm, *Phys. Rev. Lett.* **106**, 115304 (2011).
  - [16] T. Bourdel, J. Cubizolles, L. Khaykovich, K. M. F. Magalhães, S. J. J. M. F. Kokkelmans, G. V. Shlyapnikov, and C. Salomon, *Phys. Rev. Lett.* **91**, 020402 (2003).
  - [17] C. Cao, E. Elliott, H. Wu, and J. E. Thomas, *New Journal of Physics* **13**, 75007 (2011).
  - [18] E. Elliott, J. A. Joseph, and J. E. Thomas, *Phys. Rev. Lett.* **112**, 040405 (2014).
  - [19] J. A. Joseph, E. Elliott, and J. E. Thomas, *Phys. Rev. Lett.* **115**, 020401 (2015).
  - [20] E. Elliott, J. A. Joseph, and J. E. Thomas, *Phys. Rev. Lett.* **113**, 020406 (2014).
  - [21] G. E. Astrakharchik, J. Boronat, J. Casulleras, and S. Giorgini, *Phys. Rev. Lett.* **93**, 200404 (2004).
  - [22] H. Hu, A. Minguzzi, X.-J. Liu, and M. P. Tosi, *Phys. Rev. Lett.* **93**, 190403 (2004).
  - [23] X.-C. Yao, H.-Z. Chen, Y.-P. Wu, X.-P. Liu, X.-Q. Wang, X. Jiang, Y. Deng, Y.-A. Chen, and J.-W. Pan, *Phys. Rev. Lett.* **117**, 145301 (2016).
  - [24] H.-Z. Chen, X.-C. Yao, Y.-P. Wu, X.-P. Liu, X.-Q. Wang, Y.-X. Wang, Y.-A. Chen, and J.-W. Pan, *Phys. Rev. A* **94**, 033408 (2016).
  - [25] H.-Z. Chen, X.-C. Yao, Y.-P. Wu, X.-P. Liu, X.-Q. Wang, Y.-A. Chen, and J.-W. Pan, *Applied Physics B* **122**, 281 (2016).
  - [26] W. Ketterle and N. J. V. Druten (Academic Press, 1996) pp. 181–236.
  - [27] A. V. Shytov, *Phys. Rev. A* **70**, 052708 (2004).
  - [28] A. Altmeyer, S. Riedl, C. Kohstall, M. J. Wright, R. Geursen, M. Bartenstein, C. Chin, J. H. Denschlag, and R. Grimm, *Phys. Rev. Lett.* **98**, 040401 (2007).
  - [29] C. Menotti, P. Pedri, and S. Stringari, *Phys. Rev. Lett.* **89**, 250402 (2002).
  - [30] H. Heiselberg, *Phys. Rev. Lett.* **93**, 040402 (2004).
  - [31] H. Hu, X.-J. Liu, and P. D. Drummond, *New Journal of Physics* **12**, 63038 (2010).
  - [32] Y. Nishida, S. Moroz, and D. T. Son, *Phys. Rev. Lett.* **110**, 235301 (2013).
  - [33] C. Gao, J. Wang, and Z. Yu, *Phys. Rev. A* **92**, 020504 (2015).
  - [34] S. Deng, Z.-Y. Shi, P. Diao, Q. Yu, H. Zhai, R. Qi, and H. Wu, *Science* **353**, 371 (2016).